Approaching the power limit of an electrodynamic WPTS with nearly coupling-independent operation

Binh Duc Truong and Shad Roundy
Department of Mechanical Engineering, University of Utah, 1495 E. 100 S., 1550 MEK, Salt Lake City, UT, 84112, USA.

***Abstract*—This paper further develops a theoretical analysis on the limitation on transmitted power for a low-frequency electrodynamic wireless power transfer system (WPTS). Based on an equivalent circuit model that was experimentally verified in a previous work, we derive an explicit-form solution of the maximum possible power that can be transferred to an electrical load under a given constant B−field amplitude. The obtained results reveal the essential role of the quality factor Q of the mechanical resonator and the electromagnetic receiver. At the short-circuit (resonance) frequency, we denote these two values as Q_0 and $Q_{\mathrm{L}0}$ respectively. In particular, the maximum delivered power is a fractional function of the effective figure of merit characterized by $M_\mathrm{e} = k_\mathrm{e}^2 Q_0 Q_{\mathrm{L}0}$, where k_e is the generalized electrodynamic coupling coefficient. Larger M_e results in higher maximum output power, which then reaches and levels out at its fundamental limit when $M_\mathrm{e} \gg 1$. Motivating from that observation, we propose a simple method to improve the WPTS performance while keeping the operating frequency well below 1 kHz. This approach is referred to as a nearly coupling-independent operation.**

***Index Terms*—Electrodynamic Coupling, Low-frequency Wireless Power Transfer, Power Optimization, Physical Limitation**

NOMENCLATURE

ΔK	stiffness difference, $\Delta K = K_1 - K_0 = \Psi^2/L_0$
μ_0	permeability of free space, $\mu_0 = 4\pi \times 10^{-7}$ H/m
ω_0	short-circuit frequency, $\omega_0 = \sqrt{K_0/m}$
ω_1	open-circuit frequency, $\omega_1 = \sqrt{K_1/m}$
Ψ	electrodynamic transduction factor
τ	overall electrical time constant, $\tau = L_0/(R_\mathrm{p} + R_\mathrm{L})$
τ_L	electrical time constant of the load, $\tau_\mathrm{L} = L_0/R_\mathrm{L}$
τ_p	electrical time constant of the coil, $\tau_\mathrm{p} = L_0/R_\mathrm{p}$
b	mechanical damping coefficient
B_0	**B**−field amplitude
E	Young's modulus of material
F_0	(equivalent) force induced by magnetic field
k	electrodynamic coupling coefficient, $0 \leq k^2 \leq 1$
K_0	short circuit stiffness
K_1	open circuit stiffness
k_e	expedient coupling coefficient, $k_\mathrm{e}^2 = k^2/(1-k^2)$
L_0	clamped inductance of the electromagnetic transducer
l_e	effective length of the cantilever beam
m	effective mass of the electromagnetic transducer
M_a	permanent magnet mass
m_b	beam mass
M_r	remnant magnetic polarization
R_L	load resistance
R_p	coil parasitic resistance
V_M	volume of the magnet

This work was supported by the National Science Foundation ASSIST Nanosystems ERC under Award Number EEC-1160483.

I. INTRODUCTION

The expansive use of bioelectronic wearables and implantables is evident not only to treat health problems but also to increase life expectancy [1]. The wearables/implantables require energy to operate. However, batteries have limited-lifetime and can increase the size of the implant, and therefore trauma to the patient [2]. Transcutaneous wires to deliver power can cause infection. These issues have highlighted an urgent need to replace the traditional methods of supplying power. Wireless power transfer is one of the central technologies that has potential to overcome the battery problems [3].

The wireless power transfer applications are categorized into the near-field and far-field techniques, depending on the frequency and distance between the transmitter and the receiver [4]. The far-field range has a typical distance beyond ∼10 m, using propagating electromagnetic waves to transfer energy as radios transmit signals. This approach has limitations including that the output power is rather low and the transmission is omni-directional. The radiation of the high power radio frequency (RF) transmission can be potentially harmful to human body [5]. Thus, the far-field technique is less attractive for biomedical devices.

Near-field wireless power transfer system (WPTS) was widely studied utilizing capacitive or inductive coupling [6]. However, these devices typically operate in the frequency range of MHz, which limits the magnetic field magnitude that can be applied to humans according to safety standards [7], [8]. Challa *et. al.* proposed a WPTS using an electromagnetic transducer to convert the mechanical energy from the oscillating magnet tip mass to electrical energy [9]. A lumped-element model was developed and experimentally validated. Motivated by that work, we further investigate the optimum performance of this low-frequency structure and its upper bound. All analytical solutions are expressed as functions of non-dimensional physical parameters such as coupling coefficient and Q-factors. In this work, the applied magnetic flux density is considered as a constant.

II. MATHEMATICAL MODEL AND POWER OPTIMIZATION

Figure 1 depicts the device concept and generic model of an electrodynamic-based WPTS. The mechanical part of the

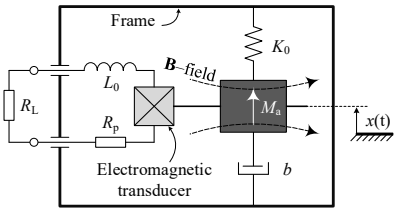

Fig. 1. Electrodynamic-based wireless power transfer concept.

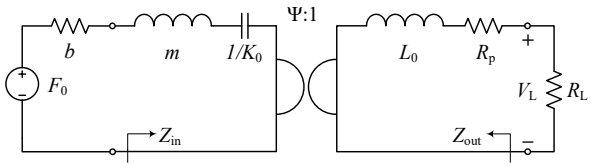

Fig. 2. Equivalent circuit model.

electromagnetic generator is characterized by a linear mass-spring-damper system. A permanent magnet M_a is placed at the tip of a cantilever beam (its magnetization direction is marked by a white arrow). When an external magnetic flux density is applied (by a transmitter coil), the interactions between the magnet and the $\mathbf{B}-$field or the magnetic flux gradient cause a moment and/or a force acting on the resonator. This mechanism results in the relative displacement $x(t)$ between the magnet and a coil that is mounted to the frame. The time-varying magnetic flux in the coil induces an electrical potential. The coupling between the mechanical and electrical domain is modeled as a linear (two-port) transducer. A portion of the electrical power is dissipated by the coil parasitic resistance. This electrical loss is inevitable and its effects on the output power is a central objective of this paper. For the sake of simplification while not losing the generality of the problem, the electrical port is typically connected to a load resistance in order to evaluate the device performance.

The equivalent circuit model of the electrodynamic WPTS is shown in Figure 2. The transducer effective mass is $m = M_\mathrm{a} + \frac{33}{140}m_\mathrm{b}$. Depending on the relative orientation between the magnet magnetization and the applied $\mathbf{B}-$field, the device operates in either torque or force mode (or even both). Details of these two configurations were presented in [9]. We now consider the case when the input current through the transmitting coil is adjusted to generate a constant amplitude of the magnetic field at a predetermined distance between the transmitter and magnet mass. The equivalent drive force has the general form of $F(t) = F_0\cos(\omega t)$ where ω is the angular frequency. The external force amplitude F_0 is a constant and is computed as

$$F_0 = \begin{cases} \dfrac{3}{2l_\mathrm{e}} M_\mathrm{r} V_\mathrm{M} \dfrac{B_0(x_0)}{\mu_0}, & \text{torque mode,} \\ \dfrac{1}{\mu_0} M_\mathrm{r} V_\mathrm{M} \dfrac{\mathrm{d}B_0(x)}{\mathrm{d}x}\Big|_{x=x_0}, & \text{force mode} \end{cases} \tag{1}$$

where $x-$axis denotes the vibration direction and $|x_0|$ is the transmission distance (from the transmitter coil). At low frequencies, the mutual inductance describing the inductive coupling between the transmitter and receiver coils is negligible. The reflected load from the magnetic onto mechanical domain is neglected due to their relatively low coupling strength. These important assumptions are used throughout the analysis. The electromagnetic transduction mechanism is represented by a gyrator. The power delivered to the resistive load is

$$P_\mathrm{L} = \frac{1}{2}\frac{|V_\mathrm{L}|^2}{R_\mathrm{L}} = \frac{1}{2}\Big(1 - \frac{\tau}{\tau_\mathrm{p}}\Big)\frac{\Delta K\omega^2\tau}{1+(\omega\tau)^2}\frac{F_0^2}{(\omega|Z_\mathrm{in}+b|)^2} \tag{2}$$

where the input impedance is given by

$$\begin{aligned} Z_\mathrm{in} &= j\Big(m\omega - \frac{K_0}{\omega}\Big) + \frac{\Psi^2}{j\omega L_0 + R_\mathrm{p} + R_\mathrm{L}} \\ &= j\Big(m\omega - \frac{K_0}{\omega}\Big) + \Delta K\frac{\tau}{1+j\omega\tau} \end{aligned} \tag{3}$$

and $1/\tau = 1/\tau_\mathrm{L} + 1/\tau_\mathrm{p}$.

In general, with arbitrary operating frequencies, the optimal load is determined by $\mathrm{d}P_\mathrm{L}/\,\mathrm{d}\tau_\mathrm{L} = 0$, which leads to

$$\begin{aligned} {}^{\mathrm{opt}}\tau_\mathrm{L} = \tau_\mathrm{p}\Big[(K_0 - m\omega^2)^2 + (\omega b)^2\Big]^{1/2} \Big/ \Big[(K_0 - m\omega^2)^2 + \\ (K_1 - m\omega^2)^2 + (\omega b)^2\big(1+(\omega\tau_\mathrm{p})^2\big) + 2\Delta K(\omega^2 b\tau_\mathrm{p})\Big]^{1/2}. \end{aligned} \tag{4}$$

It should be noted that, exactly the same result is obtained if we match the output impedance Z_out to the load, $R_\mathrm{L} = |Z_\mathrm{out}|$, where

$$Z_\mathrm{out} = j\omega L_0 + R_\mathrm{p} + \frac{\Psi^2}{j\big(m\omega - K_0/\omega\big) + b}. \tag{5}$$

At resonance frequency $\omega = \omega_0$, (4) reduces to

$${}^{\mathrm{opt}}\tau_\mathrm{L} = \frac{1}{\omega_0}\frac{1}{\sqrt{1+\big(M_0 + 1/(\omega_0\tau_\mathrm{p})\big)^2}}. \tag{6}$$

The parameter $M = \Delta K/(\omega b)$ is a resonator figure of merit [10]. Since $\Delta K = k^2K_1$, we can write $M = k^2Q_1\omega_1/\omega$ or $M = k_\mathrm{e}^2Q_0\omega_0/\omega$ where the $Q-$factors are $Q_0 = m\omega_0/b$ and $Q_1 = m\omega_1/b$ [11]. Denote $M|_{\omega=\omega_0} = M_0$, we have $M_0 = \Delta K/(\omega_0 b) = k_\mathrm{e}^2Q_0$. By introducing the coil quality factor, $Q_\mathrm{L0} = \omega_0\tau_\mathrm{p}$, (6) results in

$${}^{\mathrm{opt}}\tau_\mathrm{L} = \frac{\tau_\mathrm{p}}{\sqrt{\big(M_\mathrm{e}+1\big)^2 + Q_\mathrm{L0}^2}}. \tag{7}$$

The effective (overall) figure of merit is defined by $M_\mathrm{e} = M_0Q_\mathrm{L0} = k_\mathrm{e}^2Q_0Q_\mathrm{L0}$. The optimum delivered power is

$${}^{\mathrm{opt}}P_\mathrm{L} = \frac{1}{8}\frac{F_0^2}{b}\frac{2M_\mathrm{e}}{M_\mathrm{e}+1+\sqrt{\big(M_\mathrm{e}+1\big)^2+Q_\mathrm{L0}^2}}. \tag{8}$$

Note that $P_\mathrm{avs} = \frac{1}{8}\frac{F_0^2}{b}$ is the largest possible power that is available for transmission under a constant amplitude of the applied magnetic flux density. P_avs is also the strict upper bound that P_L can never go beyond. The ratio between the optimum output power and the input power limit is always less than unity for any physical parameters, ${}^{\mathrm{opt}}P_\mathrm{L}/P_\mathrm{avs} < 1$. This is due to the effect of the parasitic resistance R_p of the coil. Letting $R_\mathrm{p} \to 0$ (i.e., therefore $\tau_\mathrm{p} \to \infty$) and optimizing both of the load and the driving frequency simultaneously give ${}^{\mathrm{opt}}P_\mathrm{L} = P_\mathrm{avs}$ for any $M \geq 2$.

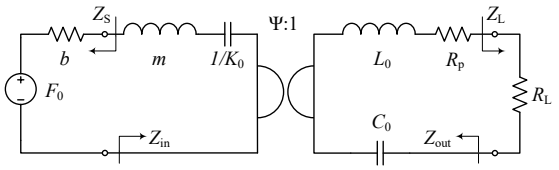

Fig. 3. Approaching the bi-conjugate impedance matching solution with an additional capacitor connected in series with the transducer coil.

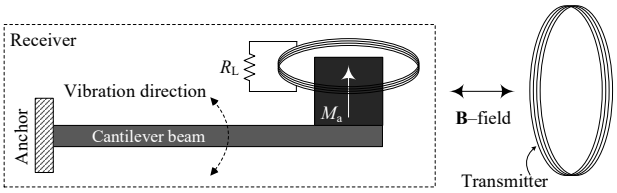

Fig. 4. Schematic of the experimental setup with the torque mode configuration conducted in [9].

III. Approximated Transmission Limitation

Given the fact that impedance matching to the load only, $R_L = |Z_{out}|$, is not the complete condition for maximizing the transferred power [12]. Larger mismatch between the input impedance and the parasitic damping coefficient, b, causes more dissipated power in the mechanical domain and less power input to the network. In principle, the bi-conjugate impedance matching condition is summarized as follows

$$Z_{in} = Z_L^* \text{ and } Z_{out} = Z_S^* \tag{9}$$

where Z_S and Z_L are general complex forms of the source and load impedances respectively. For the particular case we are considering, $\Im\{Z_S\} = \Im\{Z_L\} = 0$, $\Re\{Z_S\} = b$ and $\Re\{Z_L\} = R_L$. The impedance relations in (9) becomes

$$\Im\{Z_{in}\} = \Im\{Z_{out}\} = 0, \tag{10}$$

$$\Re\{Z_{in}\} = b, \tag{11}$$

$$\Re\{Z_{out}\} = R_L. \tag{12}$$

Since mass-spring-damper is an inseparable system with given impedance characteristics, using reactive component(s) connected to the electrical terminals would seem to be the more common point of view for the purpose of impedance matching. The simplest method is to add an external capacitor (denoted as C_0) in series with the coil L_0, as seen in Figure 3. We then choose C_0 such that $\omega_0 = \sqrt{K_0/m} = 1/\sqrt{L_0 C_0}$ and operate the WPTS at ω_0. It is obvious to see that, this technique fulfills condition (10). The solution of (12) leads to

$${}^{\text{opt}}\tau_L = \frac{\tau_p}{1 + \Psi^2/(bR_p)} = \frac{\tau_p}{1 + M_e}. \tag{13}$$

It is essential to note that, by definitions $k^2 = \Psi^2/(K_1 L_0)$, or equivalently $\Psi^2 = k_e^2 K_0 L_0 = k_e^2 m\omega_0^2 L_0$, which makes

$$\frac{\Psi^2}{bR_p} = k_e^2\left(\frac{m\omega_0}{b}\right)\left(\frac{\omega_0 L_0}{R_p}\right) = k_e^2 Q_0 Q_{L0} = M_e. \tag{14}$$

Substituting (13) into Z_{in}, the mismatch factor between $\Re\{Z_{in}\}$ and b is characterized by the ratio

$$M_s = \Re\{Z_{in}\}/b = M_e/(M_e + 2). \tag{15}$$

For moderate coupling, $M_e \gg 2$, thus $M_s \approx 1$ and $\Re\{Z_{in}\} \approx b$. This means that the condition (11) is nearly satisfied. The maximum possible power that can be transferred to the load (i.e., the output power limit) is approximated as

$${}^{\lim}P_L = P_{avs}\frac{M_e}{M_e + 1}. \tag{16}$$

TABLE I
Experimental Values of Electrical and Mechanical Parameters Used in [9].

Parameter	L_0	R_p	K_0	m	b
Value	6.4 mH	20 Ω	461 N/m	6.82 g	10.9e-3 Ns/m

From mathematical standpoint, (8) and (16) show that ${}^{\text{opt}}P_L <^{\lim} P_L$ due to $Q_{L0} > 0$. However, at low frequencies, the quality factor of the coil is much smaller than the effective figure of merit, therefore, ${}^{\text{opt}}P_L \approx^{\lim} P_L$. Obviously, large M_e is essential for increasing both the output power limit and the optimum output power.

IV. Experimental Data and Discussion on Nearly Coupling-Independent Operation

Figure 4 depicts a schematic of the experimental setup presented by Challa *et. al.* in [9], which operates in the torque mode configuration. A multi-layer solenoid was used as a transmitter. The receiver consists of an electrical coil and an Aluminum cantilever beam with an NdFeB permanent magnet attached on its tip. The coil and magnet are placed in close proximity to each other. Details of material properties and geometries of the two coils are taken from [9]. Values of relevant system parameters were extracted from their measurements and are listed in Table I. The lumped-parameter model shown in Figure 2 is an accurate representation based on the experimental validation done in [9]. All these data are used as realistic inputs for further theoretical analysis of the equations derived in previous sections.

In order to enlarge the effective figure of merit, we have three options, either increasing (i) the coupling coefficient k^2, (ii) the quality factor of the coil at the receiver Q_{L0} or (iii) the mechanical resonator quality factor Q_0. However, there is a trade-off between (i) and (ii). A larger coupling strength requires a larger number of turns of the secondary coil, which leads to higher parasitic resistance and lower coil quality factor [13]. Therefore, improving the mechanical quality factor of the cantilever beam, which is independent of (i) and (ii), could be more appropriate. The well-known formula for estimating the bending stiffness of a cantilever beam is

$$K_0 = Ewt^3/(4l_e^3). \tag{17}$$

Here, E is the Young's modulus of the beam material (e.g., for the Aluminum used in [9], $E_{Al} = 69$ GPa). w and t are the width and thickness respectively. A simple and effective

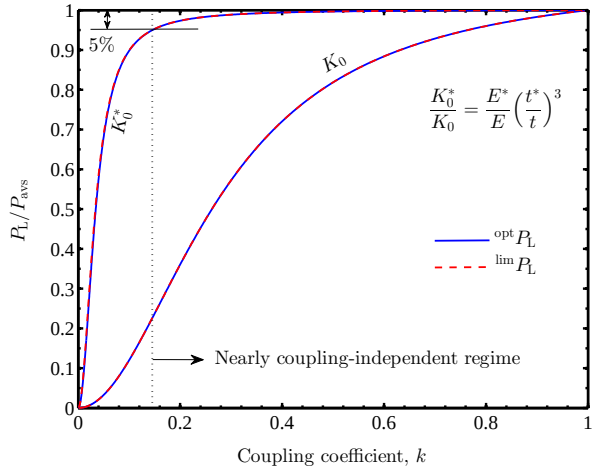

Fig. 5. Solutions of the optimum output power $^{\text{opt}}P_{\text{L}}$ and its limit $^{\text{lim}}P_{\text{L}}$ as functions of the coupling coefficient, computed by (8) and (16) respectively. Two different values of the beam stiffness are utilized: (a) K_0 taken from Table I, which is extracted from experiments done by the authors of [9], and (b) K_0^*, a suggested design of an alternative thickness $t^* = 2.5t$ and the use of Beryllium instead of Aluminum, in which $E^* = E_{\text{Be}} = 287$ GPa.

method to enhance Q_0 is to increase the mechanical resonance frequency ω_0 by using a thicker beam with higher Young's modulus material. The mechanical damping coefficient is considered unchanged for the same w and l_{e}. The change in beam mass, $\Delta m_{\text{b}} = m_{\text{b}}^* - m_{\text{b}}$ is negligibly small compared to the given magnet mass M_{a} and the effective mass m, $m \approx M_{\text{a}} \gg \Delta m_{\text{b}}$.

Figure 5 shows the changes of the maximum output power $^{\text{opt}}P_{\text{L}}$ and the highest transferable power $^{\text{lim}}P_{\text{L}}$. Here, $^{\text{opt}}P_{\text{L}}$ is obtained with the optimal load at resonance frequency, and $^{\text{lim}}P_{\text{L}}$ is achieved by approaching the bi-conjugate impedance matching conditions. Both are expressed as functions of the electrodynamic coupling coefficient $k \in [0, 1]$ and given by (8) and (16) respectively. $^{\text{opt}}P_{\text{L}}$ and $^{\text{lim}}P_{\text{L}}$ are almost identical. In order to highlight the essential role of the mechanical resonator quality factor, two different alternatives of the cantilever beam stiffness are investigated: (a) an experimentally extracted value, K_0 [9], and (b) the spring constant K_0^* of a proposed example-design with thicker beam (i.e., $t^* = 2.5t$). In addition, Aluminum is replaced by Beryllium where $E_{\text{Be}} = 287$ GPa. Note that, the mass densities of the two materials Aluminum and Beryllium are 2.7 g/cm^3 and 1.85 g/cm^3 respectively. The beam mass only increases by a factor of 1.7, which can be considerably neglected. Thus, the stiffness ratio is approximated as $K_0^*/K_0 = 65$. The corresponding resonance frequencies of the two cases are $f_0 = 41.38$ Hz and $f_0^* = 333.58$ Hz, both are far below 1 kHz. The other parameters are taken from Table I. The example system with K_0^* outperforms that of with K_0. Furthermore, for all $0.145 \leq k \leq 1$, the discrepancy between $^{\text{opt}}P_{\text{L}}$ and P_{avs} is always less than 5 %, therefore we refer this regime to as *nearly coupling-independent operation*. These findings show a comprehensive picture of the theoretical analyses in Sections II and III. According to the IEEE magnetic field safety limits, the maximum allowable field at $f_0^* = 333.58$ Hz is 1 mT [7], [8]. The corresponding optimum output power under that **B**−field amplitude is about 75.2 mW.

V. Conclusions

We derived the explicit closed-form solutions of the maximum output power and its physical limitation under a constant external magnetic flux density. The former can be obtained by adapting the electrical load while operating at the resonance frequency. Both are indistinguishable from each other due to low-frequency operation. The system performance was characterized by an effective dimensionless figure of merit that is the product of the squared electrodynamic coupling coefficient, the mechanical resonator and the electromagnetic transducer quality factors. An example design of the cantilever beam was proposed, whose output power was compared to that of a realistic system reported in previous work. The comparison showed a significant improvement when increasing the resonance frequency of the beam, and therefore the quality factor of the mechanical resonator. This technique was referred to as nearly coupling-independent operation since the optimum delivered power approaches its upper bound over a wide range of the coupling strength.

References

[1] S. M. R. Islam, D. Kwak, M. H. Kabir, M. Hossain, and K. Kwak, "The internet of things for health care: A comprehensive survey," *IEEE Access*, vol. 3, pp. 678–708, 2015.

[2] P. Gerrish, E. Herrmann, L. Tyler, and K. Walsh, "Challenges and constraints in designing implantable medical ics," *IEEE Transactions on Device and Materials Reliability*, vol. 5, no. 3, pp. 435–444, Sep. 2005.

[3] J. Moore, S. Castellanos, S. Xu, B. Wood, H. Ren, and Z. T. H. Tse, "Applications of wireless power transfer in medicine: State-of-the-art reviews," *Annals of Biomedical Engineering*, vol. 47, no. 1, pp. 22–38, Jan 2019.

[4] M. Song, P. Belov, and P. Kapitanova, "Wireless power transfer inspired by the modern trends in electromagnetics," *Applied Physics Reviews*, vol. 4, no. 2, p. 021102, 2017.

[5] W. C. Brown, "The history of power transmission by radio waves," *IEEE Transactions on Microwave Theory and Techniques*, vol. 32, no. 9, pp. 1230–1242, Sep 1984.

[6] J. Dai and D. C. Ludois, "A survey of wireless power transfer and a critical comparison of inductive and capacitive coupling for small gap applications," *IEEE Transactions on Power Electronics*, vol. 30, no. 11, pp. 6017–6029, Nov 2015.

[7] IEEE, "Ieee standard for safety levels with respect to human exposure to electromagnetic fields, 0-3 khz," *IEEE Std C95.6-2002*, pp. 1–0, Oct 2002.

[8] ——, "Ieee standard for safety levels with respect to human exposure to radio frequency electromagnetic fields, 3 khz to 300 ghz," *IEEE Std C95.1-2005 (Revision of IEEE Std C95.1-1991)*, pp. 1–238, April 2006.

[9] V. R. Challa, J. O. Mur-Miranda, and D. P. Arnold, "Wireless power transmission to an electromechanical receiver using low-frequency magnetic fields," *Smart Materials and Structures*, vol. 21, no. 11, p. 115017, 2012.

[10] E. Vittoz, *Quartz and MEM Resonators*. Dordrecht: Springer Netherlands, 2010, pp. 7–22.

[11] E. Halvorsen, "Optimal Load and Stiffness for Displacement-Constrained Vibration Energy Harvesters," *ArXiv e-prints*, Mar. 2016.

[12] C. S. Kong, "A general maximum power transfer theorem," *IEEE Transactions on Education*, vol. 38, no. 3, pp. 296–298, Aug 1995.

[13] N. W. Shuo Cheng and D. P. Arnold, "Modeling of magnetic vibrational energy harvesters using equivalent circuit representations," *Journal of Micromechanics and Microengineering*, vol. 17, no. 11, pp. 2328–2335, 2007.